GEOLOGY | THE GEOLOGICAL SOCIETY OF AMERICA®

https://doi.org/10.1130/G54871.1

Manuscript received 6 May 2026
Revised manuscript received 19 June 2026
Manuscript accepted 6 July 2026

Published online 15 July 2026

© 2026 The Authors. Gold Open Access: This paper is published under the terms of the CC-BY license.

Break-back deepwater folding and thrusting at the Romanche fracture-zone termination, NE Brazil

Stefan Back[1,*], Marco Antonio Caçador Martins-Ferreira[2], and Christopher Keith Morley[3]
[1]Geological Institute, RWTH Aachen University, 52062 Aachen, Germany
[2]Institute of Geosciences, University of Brasília, Brasília, Brazil
[3]Structural Geology Services Ltd., Woodpecker Cottage, Coffinswell, Devon 4SN, UK

ABSTRACT

The Barreirinhas deepwater fold-thrust belt is located at the landward termination of the Romanche Fracture Zone (RFZ) offshore NE Brazil. 2-D and 3-D seismic-reflection analysis integrated with borehole data shows folding and thrusting in the uppermost 10 km of basin fill in an area of >1200 km². Thrust-hanging-wall anticlines are curved, up to 5 km wide and 500 m high, extending laterally >40 km. Associated thrust faults dip SW to S showing complex roots. Deformation is kilometer-scale upward and mainly backstepping.

The Barreirinhas fold-thrust belt differs from other deepwater fold-thrust belts in that it developed primarily out-of-sequence, consists of imbricated thrust-sheets bound by multi-segment faults, contains numerous backthrusts, and lacks up-dip extension and a common basal décollement. Thrust-belt shortening was >12 km in the Late Cretaceous, and <2 km in the Cenozoic. We interpret the Barreirinhas break-back fold-thrust system to result from variations in far-field stresses (Mid-Atlantic ridge-push) and strain partitioning along the RFZ.

INTRODUCTION

Passive continental margins can show compression driven by far-field stresses, as documented, for example, along the Atlantic margins offshore NW Europe (Davies et al., 2004), the USA (Kulpecz et al., 2009), offshore NE Brazil (Azevedo, 1991; Cobbold et al., 2010), Morocco (Neumaier et al., 2016), and Angola (Hudec and Jackson, 2002). Crustal-driven compression has also been documented at transform margins, along transform faults (Basile, 2015), and at ocean fracture zones (Davies et al., 2005; Nemčok et al., 2023). Until today, there have been only limited drilling campaigns and few seismic-reflection studies at intersections between passive and transform continental margins. Particularly, the landward termination of ocean fracture zones remains poorly constrained, mainly due to deep burial by a thick sedimentary cover.

Recent publication of industry seismic-reflection data offers new opportunities to investigate continental margin intersections. This study describes a combined 2-D and 3-D seismic-reflection dataset from the Equatorial Atlantic margin offshore NE Brazil that images the landward termination of the Romanche Fracture Zone (RFZ; Fig. 1). The data reveal evidence for contractional tectonics along the RFZ between the Late Cretaceous and today. The data image a deepwater fold-thrust belt (Conti and Chira Oliva, 2021) that developed primarily as a break-back system, i.e., with deformation migrating toward the continental hinterland (out-of-sequence, sensu Morley, 1988). The documented system is an exceptional example of break-back folding and thrusting outside of a convergent margin.

DATA AND GEOLOGIC SETTING

The study area is located ~50–200 km offshore the NE coast of Brazil at the landward termination of the RFZ (Fig. 1A). The 2-D seismic-reflection data are from the Grand-North multichannel seismic survey with 14 s two-way time (TWT) recording length (Fig. 1B). The 3-D seismic-reflection data are from survey BM-BAR-1 (Block of the Barreirinhas Basin survey; Figs. 1A and 2) with 6 s TWT recording length. The seismic data were depth-converted based on velocity data from offshore boreholes (Fig. 1A). The present-day water depth of the study area is between 50 m on the shelf and 3.2 km in the deeper basin areas. The basement is buried ~8–15 km below sea level (Fig. 1B). Tamara et al. (2020) and Aslanian et al. (2021) interpreted the region N and NE of the study area (Fig. 1A) as highly extended continental crust.

The RFZ (Fig. 1) initiated as an intracontinental shear zone in the Early Cretaceous (ca. 140 Ma; Müller et al., 2019; Montenegro et al., 2021; de Castro et al., 2024). Davison et al. (2016) interpreted dextral transtensional rifting in the Aptian along the fracture zone, followed by Albian compression. Müller et al. (2019), Tavares et al. (2020), and Nemčok et al. (2023) interpreted continental breakup, seafloor spreading, and transform faulting between ca. 110 Ma and 90 Ma. Nemčok et al. (2013) and Tavares et al. (2020) interpreted a change of stress conditions at the RFZ ca. 84 Ma due to an orientation change of the Mid-Atlantic Ridge spreading center. At present, the RFZ forms ridges in the Equatorial Atlantic (Fig. 1A) that rise up to ~2.5 km above the surrounding basins.

Numerous seamounts occur offshore NE Brazil, some of which define the boundary between extended continental and oceanic crust (Tavares et al., 2020; Aslanian et al., 2021; Santos et al., 2021, 2022; de Castro et al., 2024). Volcanic chains form a rhomboid pattern parallel to the passive (NW-SE) and transform (W-E) continental margin (Fig. 1A). The seamounts closest to the study area are dated 65–14 Ma (Santos et al., 2021).

SEISMIC INTERPRETATION

2-D seismic-reflection data (Fig. 1B) image the deeper crustal structure of the continental margin near the landward termination of the RFZ. The margin shows deep-rooted, steep, upward branching, widening and outward flattening faults, of which some underlie hanging-wall anticlines up to 5 km wide. Landward-

Stefan Back https://orcid.org/0000-0003-3134-3367
*back@geol.rwth-aachen.de

CITATION: Back, S., et al., 2026, Break-back deepwater folding and thrusting at the Romanche fracture-zone termination, NE Brazil: Geology, v. 54, p. 1027–1032, https://doi.org/10.1130/G54871.1

Downloaded from pubs.geoscienceworld.org/gsa/geology/article-pdf/54/10/1027/8317041/g54871.1.pdf by RWTH Aachen University user on 17 November 2026

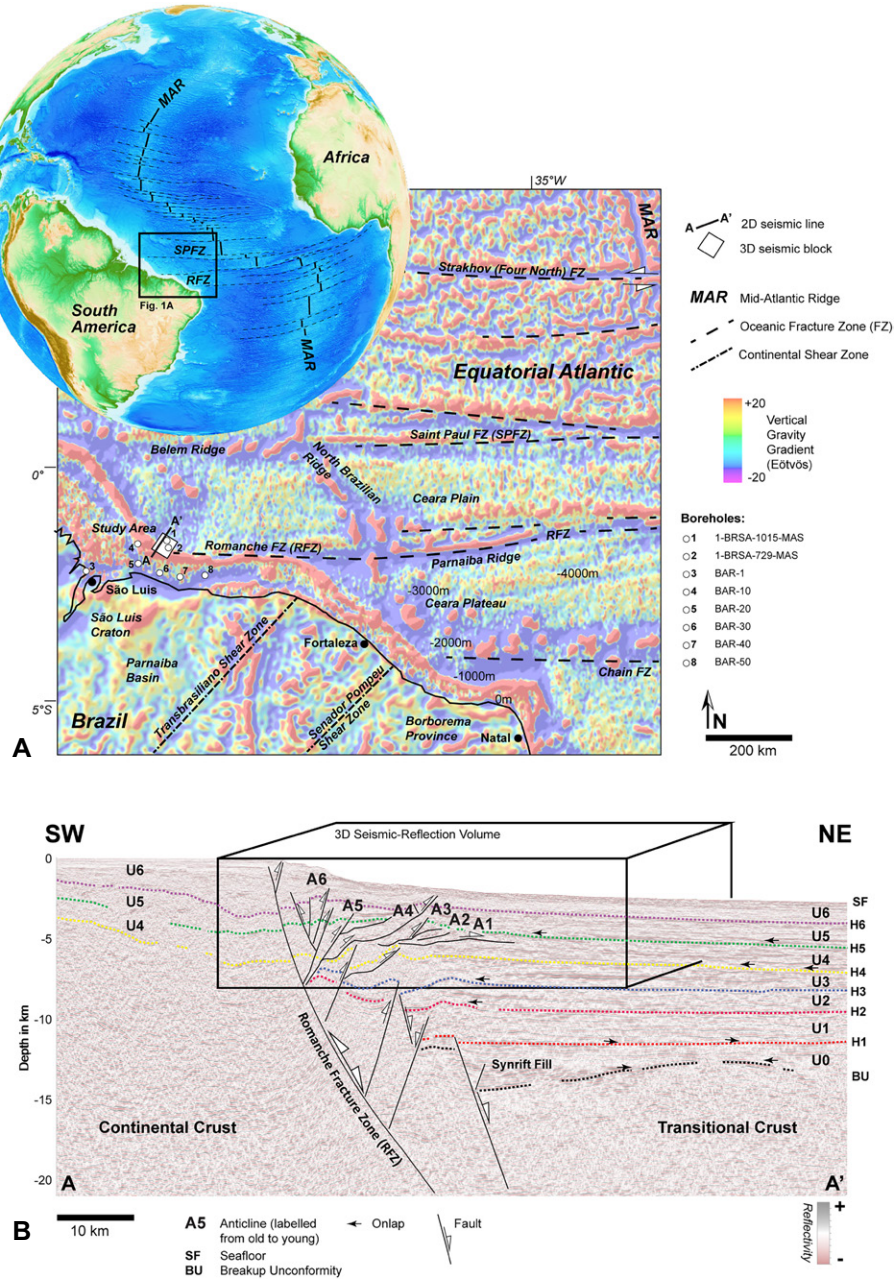


Figure 1. Study area offshore NE Brazil. Bathymetry and topography from Tozer et al. (2019). (A) Vertical-gravity gradient map (Sandwell et al., 2014) with highest values (red) offshore at continental slope, seamounts, and ridges along oceanic fracture zones. Main basins, geological provinces, and shear zones shown onshore. (B) Depth-converted 2-D seismic-reflection line Grand North 0239-0260 across Romanche Fracture Zone (RFZ); horizon and fault interpretation. Barreirinhas fold-thrust belt located in the upper 8 km of sedimentary section. For uninterpreted seismic data, see Fig. S1 in the Supplemental Material[1].

dipping faults of various angles connect to deeper-seated branches of a major seaward-dipping master fault, interpreted as a main branch of the RFZ (Fig. 1B). In the upper 8 km of section is a NE-directed fold-thrust belt that comprises several SW-dipping to sub-horizontal thrusts overlain by hanging-wall anticlines. The shallow-seated fold-thrust system is primarily out-of-sequence, i.e., the lowest and oldest deformation is most basinward, and is overlain by a succession of upward- and landward-shifting folds and thrusts (Fig. 1B).

Eight seismic horizons (BU = breakup unconformity; H1 to H6; and seafloor) and units (acoustic basement; units U0 to U6) were mapped (Fig. 1B). The acoustic basement shows a few high-amplitude, medium-continuity, low-frequency, semi-horizontal reflectors within a chaotic reflection matrix. Above, high-amplitude reflectors are onlapped at BU by U0, which is wedging into a bounding normal fault in the SW. U1 to U3 are in total up to 5 km thick and characterized by subparallel reflections of medium amplitude, frequency, and continuity, which are deformed near the fracture zone (Fig. 1B). U4 to U6 are in total 4–5 km thick and characterized by subparallel reflections of medium to high amplitude, medium frequency and medium to high continuity. Particularly, U4 is deformed by faults and folds at and basinward of the fracture-zone intersection (Fig. 1B). The series of upward- and landward-migrating anticlines A1 to A6 documents break-back folding and thrusting.

Figure 2 shows a fault map along an auxiliary 3-D horizon in the upper part of U4 (Fig. 2A) and five representative 3-D seismic-reflection lines across the study area (Figs. 2B–2F). The seismic lines are margin-parallel (B–B′) and margin-perpendicular (C–C′ to F–F′). Boreholes 1-BRSA-729-MAS and 1-BRSA-1015-MAS provide time-depth, lithological, and stratigraphic constraints. Sections C–C′ to F–F′ document that a maximum of contraction and deformation affected U4. U5 and U6 show deformation in the most landward part of the fold-thrust belt (Figs. 2B and 2E) and recent faulting and folding in an inversion zone at and above F4 in the central study area (Figs. 1B, 2A, and 2C–2E).

Faults F1 and F2 consist of multiple connected segments (Figs. 2A, 3A, and 3B) rooted in sub-horizontal to folded, high-amplitude, low-frequency reflections (Fig. 2F). F1 and F2 extend along strike over 40 km, dip up to 30° SW, and are flanked by hanging-wall anticlines A1 and A2 that are up to 5 km wide and a few hundreds of meters high. Faults F3, F4, and F5 are shorter, mostly steeper dipping up to 35°. Hanging-wall anticlines A3, A4, and A5 are only locally preserved. Young folding is observed in the hanging wall of F6 (Fig. 2F), in the thrust-belt center above reactivated fault F4 (Figs. 2C–2F), and at the southern edge of the dataset (Fig. 2A). Fault heaves are largest for F2 (>3 km) and F1 (>2 km) in direction 20°. F3, F4, and F5 have heaves between 1 km (U3) and 0.4 km (U4) in direction 30°–40°. F4 and F6 additionally displace U5 and U6 with heaves <0.5 km in directions 20°–60°. Backthrusts mainly occur on the landward flanks of A1 and A2 (Figs. 2A, 2C, 2E, 3A, and 3B). Small-scale backthrusts with a length of a few hundreds of meters and offsets <50 m occur locally on the landward flank of the recent part of inversion anticline A4 (Fig. 2D).

Line-length balancing along section F–F′ (total section length 75 km; Fig. 2F) provides a first-pass estimate of shortening by faulting and

[1]Supplemental Material. Figure S1: Uninterpreted seismic-reflection sections A–A′ (Fig. 1B), B–B′ (Fig. 2B), C–C′ (Fig. 2C), D–D′ (Fig. 2D), E–E′ (Fig. 2E), and F–F′ (Fig. 2F). Please visit https://doi.org/10.1130/GEOL.S.32940182 to access the supplemental material; contact editing@geosociety.org with any questions.

Downloaded from pubs.geoscienceworld.org/gsa/geology/article-pdf/54/10/1027/8317041/g54871.1.pdf by RWTH Aachen University user on 17 November 2026

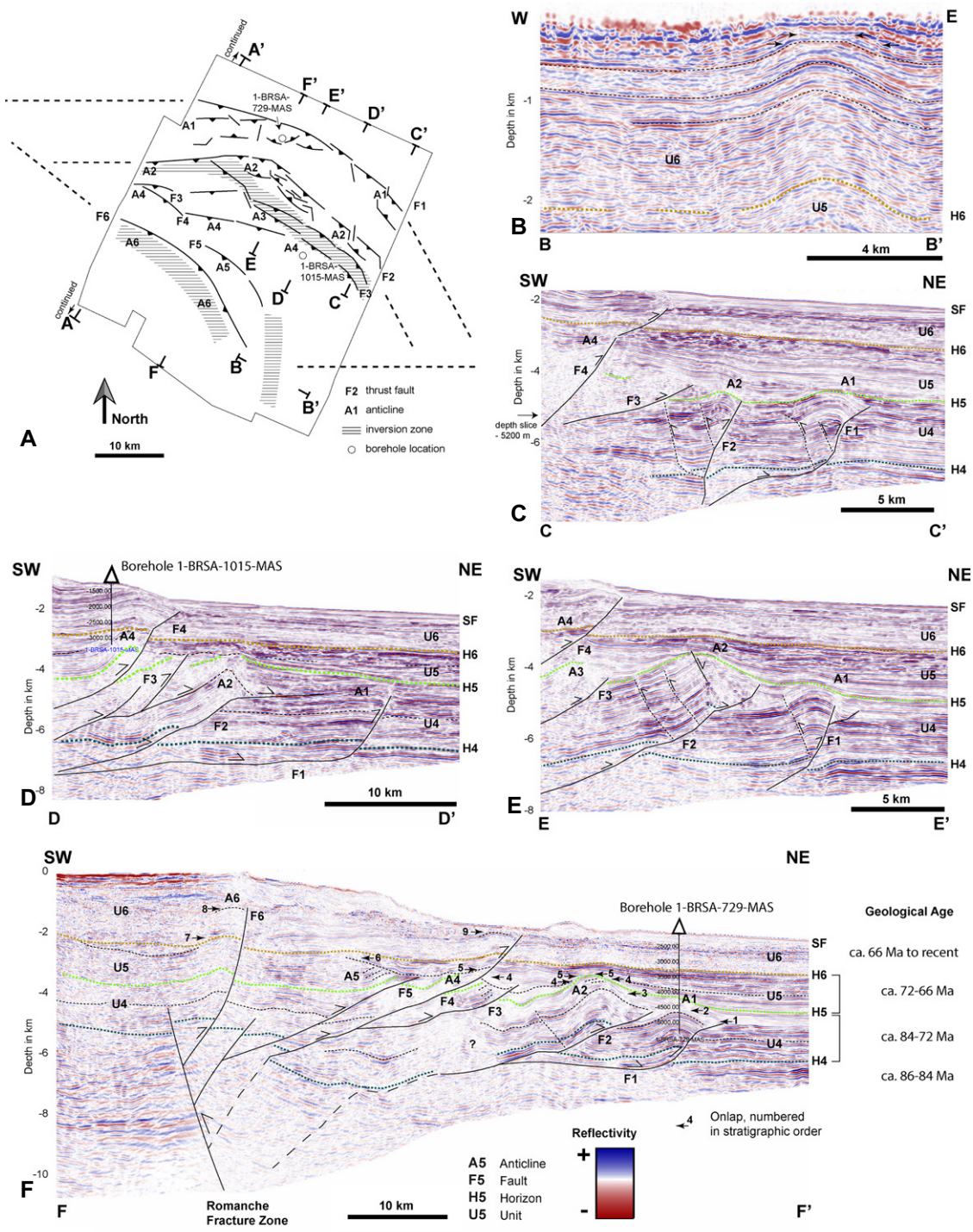


Figure 2. (A) Structural overview along 3-D horizon in the upper part of U4. (B–F) Representative seismic-reflection sections across Barreirinhas fold-thrust belt. Section B–B′ shows modern folding in E-W direction. Sections C–C′ to F–F′ document maximum of contractional deformation in U4. Note consequent break-back architecture of fold-thrust system, irregular décollement zone, and the occurrence backthrusts. Recent folding affects the modern seafloor in B, D, and E. For uninterpreted seismic data, see Fig. S1 (footnote 1).

folding of U4 of >12 km. Shortening thereafter is <2 km, mainly affecting U6, concentrating on three distinct inversion zones in the S, SW, and center of the study area (Fig. 2A).

GEOLOGIC INTERPRETATION

Biostratigraphic and thermochronological analyses of core samples from wells BAR-1, BAR-10, BAR-20, BAR-30, BAR-40, and BAR-50 (Fig. 1A; Fellin et al., 2024) provide a Santonian age (ca. 86–84 Ma) for top U3, a Campanian age (ca. 84–72 Ma) for U4, and a Maastrichtian age (ca. 72–66 Ma) for U5. Units U2 and U3 show bent reflections near the RFZ (Fig. 1B) due to folding. Maximum thrust and fold activity occurred within U4 (Figs. 1B and 2C–2F). Reflection terminations on top of A2 and reflection wedges on the flanks of A1 and A2 document syn-tectonic deposition during U4 times. U5 is less affected by faulting and folding. Reflection terminations at the base and within U5 show that A3, A4, and A5 are largely eroded and that U5 onlaps the remnant fold-thrust system. U6 is displaced by reactivation of F4 in the central fold-thrust belt, affected by folding above F6 and the growth of a N-S–oriented anticline in the southern part of the study area. In places, deformation of U6 reaches the seafloor (Figs. 2B, 2D, and 2E).

Figure 3 shows that F1 and F2 are multisegment en echelon faults connected by oblique step-overs, over distances of kilometers (Fig. 3A) to tens of kilometers (Fig. 3B). A similar rhomboid geometry is imaged at the scale of hundreds of kilometers between the RFZ and the Saint Paul Fracture Zone (Fig. 3C). The

Downloaded from pubs.geoscienceworld.org/gsa/geology/article-pdf/54/10/1027/8317041/g54871.1.pdf by RWTH Aachen University user on 17 November 2026

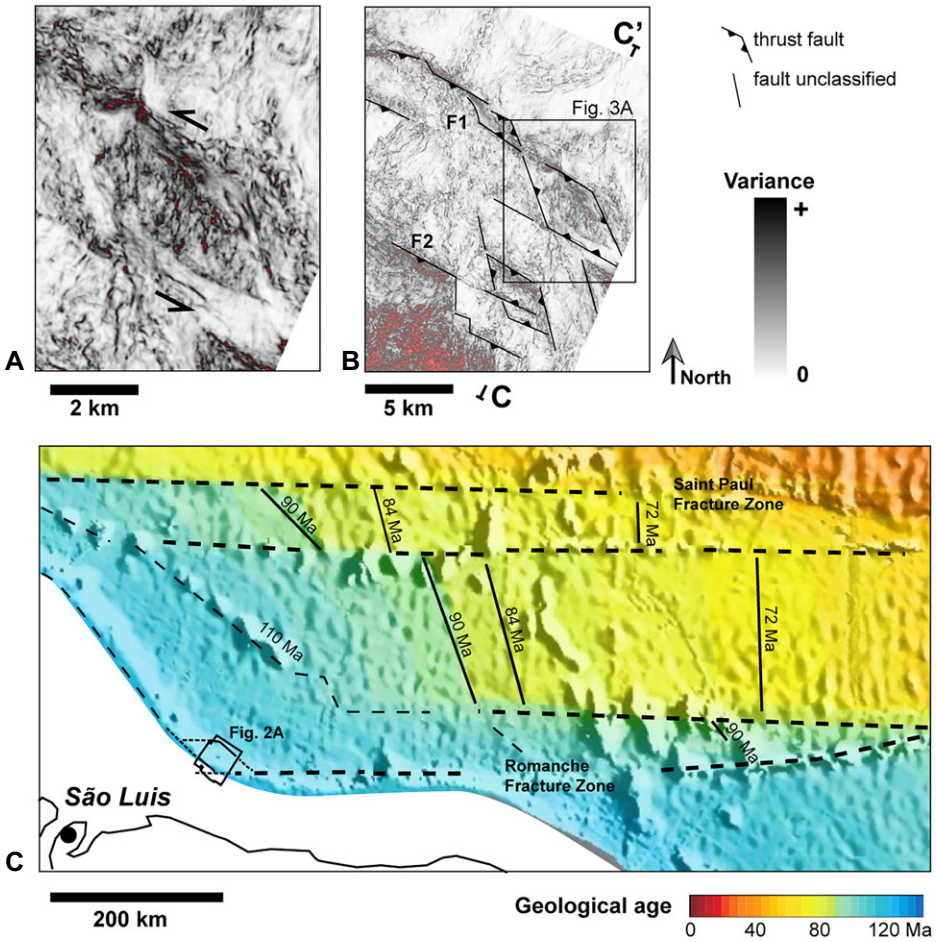


Figure 3. (A) Variance depth-slice at −5200 m showing rhomboid structure interpreted as strike-slip duplex, contractional between 84 Ma and 72 Ma. (B) Zoom-out of depth-slice providing overview on multi-segment faults enclosing push-up blocks. Fault-bound low-variance areas coincide with flat spots (see Fig. 2C). (C) Study area at Romanche Fracture Zone to divergent-margin intersection, and geological age of seafloor (Gee and Kent, 2007; Channell, 1995).

structural grain of the study area is interpreted as initially transtensional during breakup and transform faulting (Fig. 4). Then, between ca. 90 Ma and 84 Ma, inversion affected the main landward fault of the RFZ. Around 84 Ma, the Mid-Atlantic Ridge spreading-center changed orientation (Nemčok et al. 2013) from oblique to perpendicular to the RFZ (Tavares et al., 2020), and the resulting stress change is interpreted to have caused growth of F1. Between 84 Ma and 72 Ma, clockwise stress rotation is interpreted to have shifted thrusting and folding successively landward, ultimately concentrating on the main RFZ bounding fault (Fig. 4). The fold-thrust belt was tectonically dormant thereafter until the main RFZ bounding fault and fault F4 in the center were reactivated in recent times.

DISCUSSION

Deepwater fold-thrust belts can be classified between two end members, near-field stress-driven systems confined to the sedimentary section, and basement-controlled systems driven by far-field stresses (Morley et al. 2011). Krueger et al. (2012) and Tamara et al. (2020) interpreted deepwater thrusting and folding immediately north of the study area as near-field gravity-driven, as documented by up-dip extensional faults balanced down-dip by compressional structures above a seaward-dipping detachment. Key differences of the Barreirinhas fold-thrust belt to these systems are the absence of updip extensional faults; the lack of a common basal décollement; the succession of landward-migrating, up-building, break-back thrusts and folds; the complex fault-framework formed by multi-segmented faults linked by step-overs, including the presence of numerous backthrusts and push-up blocks; the Holocene reactivation and folding in the center and along the southern edges of the fold-thrust belt; and the documentation of deep-seated faults and folds beyond 3-D seismic penetration (Fig. 1B) that indicate basement-rooted deformation.

Deepwater fold-thrust belts entirely driven by far-field stresses typically exhibit landward-dipping detachments, which can be best observed at convergent margins (e.g., Xia et al., 2023; Eickhoff et al., 2025). Key differences of the Barreirinhas fold-thrust belt to subduction- and collision-related systems are the absence of any significant décollement; the limited lateral (~40 km) and basinward (~30 km) extent of contraction; the low (<15 km) amount of cumulative horizontal shortening; and the multi-segment, en echelon architecture of the main thrust faults. Figures 2 and 3 show the Barreirinhas thrust belt built by contractional duplexes of varying sizes, comprising a complex association of folds, thrust faults, backthrusts, and local push-up blocks. Contraction is generally in bends from W to NW. The location of the fold-thrust belt in an "inner-corner transform-divergent margin intersection" (sensu Basile, 2015; Fig. 3C) is sensitive to changes in far-field stress and structural reactivation. The large basin between the RFZ and the Saint Paul Fracture Zone is that of a giant pull-apart structure likely formed in the early times of rifting and seafloor-spreading (Davison et al., 2016). The contractional tectonics documented in this study mainly occurred between 84 Ma and 72 Ma (Fig. 4). Nemčok et al. (2013) and Tavares et al. (2020) interpreted at this time a significant change in plate motion in the Equatorial Atlantic associated with an orientation change of the Mid-Atlantic Ridge spreading center from oblique to orthogonal to the RFZ. We interpret a variable far-field stress regime related to changing ocean-spreading parameters (ridge push) and strain partitioning along the RFZ as key factors driving break-back tectonics in the Barreirinhas fold-thrust system.

The Barreirinhas fold-thrust system has the greatest similarities in (1) relationship to large-displacement strike-slip faults, (2) overall dimensions, (3) thick-skinned core, thin-skinned outer zone structures, (4) development in a significantly evolving stress field with time, and (5) similar map view geometries, with transpressional fold-thrust belts along the Nayband fault, Tabas Block, Central Iran (Konon et al., 2016, 2026), and in West Spitzbergen (e.g., Bergh et al., 1997, Leever et al., 2011). The Tabas Block example involves an intracontinental strike-slip fault, so the plate setting is different, but deformation is geometrically very similar. West Spitzbergen involves a transform margin, but transpressional shortening is greater (20–40 km) and there is a collisional component. Strain partitioning in West Spitzbergen evolved with time and became more pronounced (Leever et al., 2011). The Tabas fold belt developed at a restraining bend in the north of the Nayband fault, and structural development youngs from most external toward the main strike-slip fault (Konon et al., 2026). The location of the Barreirinhas fold-thrust belt at the transform-divergent margin intersection represents a third variant on where thick-thin-skinned fold-thrust belts can develop; it covers the smallest area and is the

Downloaded from pubs.geoscienceworld.org/gsa/geology/article-pdf/54/10/1027/8317041/g54871.1.pdf by RWTH Aachen University user on 17 November 2026

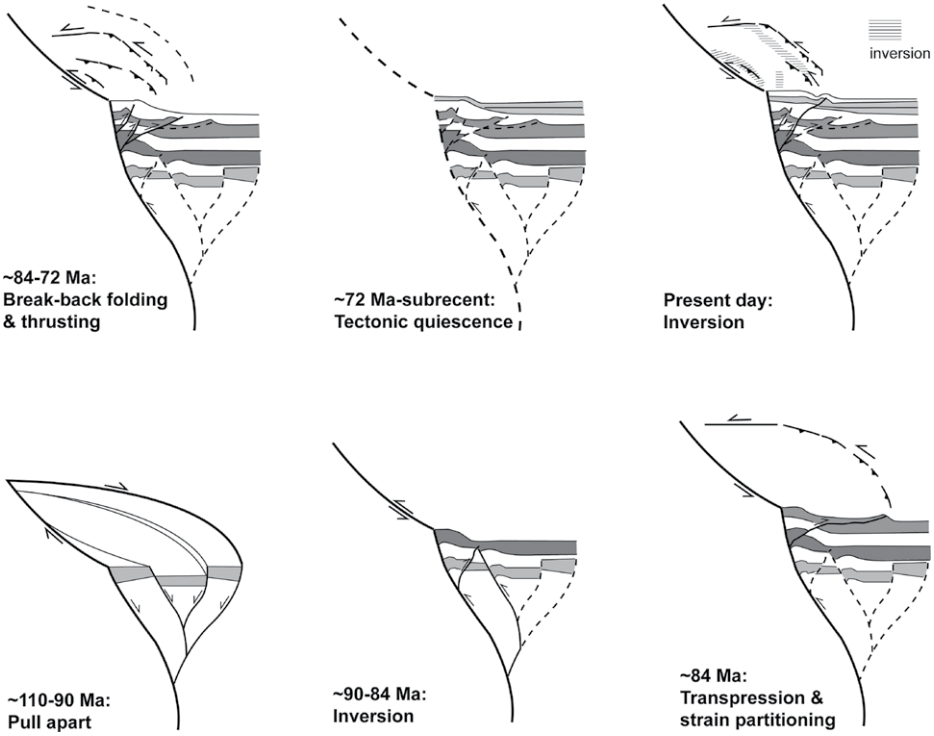


Figure 4. Schematic interpretation of Romanche Fracture Zone (RFZ) study area between 110 Ma and today. Contractional tectonics occurred primarily between 84 Ma and 72 Ma caused by changing ocean-spreading parameters (ridge push) and strain partitioning along RFZ.

least structurally complex of the three. Similar systems potentially occur at other passive-transform margin intersections, including western equatorial Africa (Briggs et al. 2009; Fig. 1). Yet, in such sediment-rich settings these systems will be buried deeply and therefore more difficult to detect and image.

CONCLUSIONS

This study documents a unique break-back deepwater fold-thrust belt at the landward termination of a major fracture zone at the Brazilian passive margin. Deformation within the Barreirinhas fold-thrust system is dominantly upward back-building, accommodating a total shortening of <15 km. The fold-thrust system is interpreted as driven by contraction caused by a change in orientation of Mid-Atlantic spreading between 84 Ma and 72 Ma. The break-back architecture of the system likely results from variable strain partitioning in a rotating stress field. We suspect the occurrence of similar basement-controlled contractional belts at other intersections between fracture zones and divergent margins, likely hidden beneath a thick sedimentary cover or superimposed gravity-driven mass-transport systems.

ACKNOWLEDGMENTS

We thank ANP for seismic and borehole data; Schlumberger for academic licensing of Petrel software; the Alexander von Humboldt Foundation and CAPES for grant BRA 1213008 HFSTCAPES-P; and C. Berndt, J. Cartwright, and R. Strachan for valuable comments.

REFERENCES CITED

Aslanian, D., et al., 2021, Deep structure of the Pará-Maranhão/Barreirinhas passive margin in the equatorial Atlantic (NE Brazil): Journal of South American Earth Sciences, v. 110, https://doi.org/10.1016/j.jsames.2021.103322.

Azevedo, R.P., 1991, Tectonic Evolution of Brazilian Equatorial Continental Margin Basins [Ph.D. thesis]: London, England, Imperial College, University of London, 455 p.

Basile, C., 2015, Transform continental margins—Part 1: Concepts and models: Tectonophysics, v. 661, p. 1–10, https://doi.org/10.1016/j.tecto.2015.08.034.

Bergh, S.G., Braathen, A., and Andresen, A., 1997, Interaction of basement involved and thin-skinned tectonism in the Tertiary fold-thrust belt of central Spitsbergen, Svalbard: AAPG Bulletin, v. 81, p. 637–661, https://doi.org/10.1306/522B43F7-1727-11D7-8645000102C1865D.

Briggs, S.E., Davies, R.J., Cartwright, J., and Morgan, R., 2009, Thrusting in oceanic crust during continental drift offshore Niger Delta, equatorial Africa: Tectonics, v. 28, TC1004, https://doi.org/10.1029/2008TC002266.

Channell, J.E.T., 1995, Recalibration of the geomagnetic polarity timescale: Reviews of Geophysics, v. 33, p. 161–168, https://doi.org/10.1029/95RG00404.

Cobbold, P.R., Gilchrist, G., Scotchman, I., Chiossi, D., Fonseca Chaves, F., Gomes de Souza, F., and Lilletveit, R., 2010, Large submarine slides on a steep continental margin (Camamu Basin, NE Brazil): Journal of the Geological Society, v. 167, p. 583–592, https://doi.org/10.1144/0016-76492009-033.

Conti, A.F., and Chira Oliva, P.A., 2021, An integrated approach for reservoirs characterization: A case study from the Barreirinhas basin in Maranhão, Brazil: Journal of South American Earth Sciences, v. 112, https://doi.org/10.1016/j.jsames.2021.103610.

Davies, R.J., Cloke, I., Cartwright, J., Robinson, A., and Ferrero, C., 2004, Post-breakup compression of a passive margin and its impact on hydrocarbon prospectivity: An example from the Tertiary of the Faeroe–Shetland Basin, United Kingdom: AAPG Bulletin, v. 88, p. 1–20, https://doi.org/10.1306/09030303008.

Davies, R.J., MacLeod, C.J., Morgan, R., and Briggs, S.E., 2005, Termination of a fossil continent-ocean fracture zone imaged with three-dimensional seismic data: The Chain Fracture Zone, eastern equatorial Atlantic: Geology, v. 33, p. 641–644, https://doi.org/10.1130/G21530.1.

Davison, I., Faull, T., Greenhalgh, J.O., Beirne, E., and Steel, I., 2016, Transpressional structures and hydrocarbon potential along the Romanche Fracture Zone: A review, *in* Nemčok, M., et al., eds., Transform Margins: Development, Controls and Petroleum Systems: Geological Society, London, Special Publication 431, p. 235–248, https://doi.org/10.1144/SP431.2.

de Castro, D.L., Oliveira, D.C., and Bezerra, H.R., 2024, Evolution of the transtensional Barreirinhas pull-apart system in the Brazilian Equatorial margin and its correlation with the African conjugate counterpart: Tectonophysics, v. 889, https://doi.org/10.1016/j.tecto.2024.230470.

Eickhoff, D., Back, S., Reicherter, K., and Ritter, J.R.R., 2025, Seismic reprocessing of BELCORP-DEKORP 1A reveals deep fault reflections of the Paleozoic Eifel Fold and Thrust Belt in Germany: Tectonophysics, v. 903, https://doi.org/10.1016/j.tecto.2025.230702.

Fellin, M.G., Zattin, M., Zuffa, G.G., De Ros, L.F., Cupertino, J.A., Schiffer de Souza, R., Morais Neto, J.M., and Dalmonte, C., 2024, New detrital petrographic and thermochronologic constraints on the Late Cretaceous–Neogene erosional history of the equatorial margin of Brazil: Implications for the surface evolution of a complex rift margin: Basin Research, v. 36, https://doi.org/10.1111/bre.12808.

Gee, J., and Kent, D., 2007, Source of oceanic magnetic anomalies and the geomagnetic polarity timescale, *in* Kono, M., and Schubert, G., eds., Treatise on Geophysics: Geomagnetism: Amsterdam, Elsevier, v. 5, p. 455–507.

Hudec, M.R., and Jackson, M.P.A., 2002, Structural segmentation, inversion and salt tectonics on a passive margin: Evolution of the Inner Kwanza Basin, Angola: Geological Society of America Bulletin, v. 114, p. 1222–1244, https://doi.org/10.1130/0016-7606(2002)114<1222:SSIAST>2.0.CO;2.

Konon, A., Nadimi, A., Koprianiuk, M., Wysocka, A., Szaniawski, R., Wyglądała, M., Slaby, E., Beygi, S., and Barski, M., 2016, Formation of intracontinental basins in the opposite corners of the Tabas block as coeval structures controlled by transpressional faulting, Iran: Geological Society of America Bulletin, v. 128, p. 1593–1617, https://doi.org/10.1130/B31362.1.

Konon, A., Nadimi, A., Mikolajczak, M., Rybak-Ostrowska, B., Wyglądała, M., and Bouzari, S., 2026, Late Pliocene to Quaternary evolution of the Shotori strike-slip deformation belt: The interplay between thin- and thick-skinned tectonics along the border between the Tabas and Lut blocks, Iran: Geological Society of America Bulletin, https://doi.org/10.1130/B38584.1.

Krueger, A., Murphy, M., and Burke, K., 2012, Deposition and deformation in the deepwater sediment of the offshore Barreirinhas Basin, Brazil: Geosphere, v. 8, p. 1606–1631, https://doi.org/10.1130/GES00805.1.

Kulpecz, A.A., Miller, K.G., Browning, J.V., Edwards, L.E., Powars, D.S., McLaughlin, P.P., Jr., Harris,

Downloaded from pubs.geoscienceworld.org/gsa/geology/article-pdf/54/10/1027/8317041/g54871.1.pdf by RWTH Aachen University user on 17 November 2026

A.D., and Feigen-Son, M.D., 2009, Post-impact deposition in the Chesapeake Bay impact structure: Variations in eustasy, compaction, sediment supply, and passive-aggressive tectonism, *in* Gohn, G.S., et al., eds., The ICDP-USGS Deep Drilling Project in the Chesapeake Bay Impact Structure: Results from the Eyreville Core Holes: Geological Society of America Special Paper 458, p. 811–837, https://doi.org/10.1130/2009.2458(34).

Leever, K.A., Gabrielsen, R.H., Faleide, J.I., and Braathen, A., 2011, A transpressional origin for the West Spitsbergen fold-and-thrust belt: Insight from analog modelling: Tectonics, v. 30, TC2014, https://doi.org/10.1029/2010TC002753.

Montenegro, C.G.L., Gomes, M.P., de Castro, D.L., Perez, Y.A., and Oliveira, D.C., 2021, The Barreirinhas Basin internal architecture and the evidence of transform movements along the Romanche Fracture Zone, Brazilian Equatorial Margin: Journal of South American Earth Sciences, v. 107, https://doi.org/10.1016/j.jsames.2020.103049.

Morley, C.K., 1988, Out-of-sequence thrusts: Tectonics, v. 7, p. 539–561, https://doi.org/10.1029/TC007i003p00539.

Morley, C.K., King, R., Hillis, R., Tingay, M., and Backe, G., 2011, Deepwater fold and thrust belt classification, tectonics, structure and hydrocarbon prospectivity: A review: Earth-Science Reviews, v. 104, p. 41–91, https://doi.org/10.1016/j.earscirev.2010.09.010.

Müller, R.D., et al., 2019, A global plate model including lithospheric deformation along major rifts and orogens since the Triassic: Tectonics, v. 38, p. 1884–1907, https://doi.org/10.1029/2018TC005462.

Nemčok, M., Henk, A., Allen, R., Sikora, P.J., and Stuart, C., 2013, Continental break-up along strike-slip fault zones; observations from the Equatorial Atlantic, *in* Mohriak, W.U., Danforth, A., Post, P.J., Brown, D.E., Tari, G.C., Nemčok, M., and Sinha, S.T., eds., Conjugate Divergent Margins: Geological Society, London, Special Publication 369, p. 537–556, https://doi.org/10.1144/SP369.8.

Nemčok, M., et al., 2023, Early post-breakup kinematic adjustments of continental–oceanic transform fault zones: Cape Range, Coromandal and Romanche transform margin case study, *in* Nemčok, M., et al., eds., History and Hydrocarbon Habitat Models of Transform Margins: Their Differences from Rifted Margins: Geological Society, London, Special Publication 524, p. 219–243, https://doi.org/10.1144/SP524-2021-110.

Neumaier, M., Back, S., Littke, R., Kukla, P.A., Schnabel, M., and Reichert, C., 2016, Late Cretaceous to Cenozoic geodynamic evolution of the Atlantic margin offshore Essaouira (Morocco): Basin Research, v. 28, p. 712–730, https://doi.org/10.1111/bre.12127.

Sandwell, D.T., Müller, R.D., Smith, W.H.F., Garcia, E., and Francis, R., 2014, New global marine gravity model from CryoSat-2 and Jason-1 reveals buried tectonic structure: Science, v. 346, p. 65–67, https://doi.org/10.1126/science.1258213.

Santos, A.C., Bonifácio, J.F., Monteiro, L.G.P., Rocha-Júnior, E.R.V., Guerra, L.S.C., Heilbron, M., Magini, C., Jeck, I.K., and Bruno, H., 2021, Brazilian Equatorial Margin: Magmatic genesis and evolution, *in* Santos, A.C., and Hackspacher, P.C., eds., Meso-Cenozoic Brazilian Offshore Magmatism: Geochemistry, Petrology, and Tectonics: Academic Press, p. 433–472, https://doi.org/10.1016/B978-0-12-823988-9.00016-2.

Santos, M., Reis, T., Silva, C.G., Gorini, M.A., and Caldas, N.A., 2022, Seismic evidences of recurrent volcanism across the North Brazilian and the Fernando de Noronha ridges—Brazilian Equatorial Atlantic Ocean: Brazilian Journal of Geophysics, v. 40, p. 1–11, https://doi.org/10.22564/brjg.v40i1.2135.

Tamara, J., McClay, K.R., and Hodgson, N., 2020, Crustal structure of the central sector of the NE Brazilian equatorial margin, *in* McClay, K.R., and Hammerstein, J.A., eds., Passive Margins: Tectonics, Sedimentation and Magmatism: Geological Society, London, Special Publication 476, p. 163–191, https://doi.org/10.1144/SP476-2019-54.

Tavares, A.C., de Castro, D.L., Bezerra, F.H.R., Oliveira, D.C., Vannucchi, P., Iacopini, D., Jovane, L., and Vital, H., 2020, The Romanche fracture zone influences the segmentation of the equatorial margin of Brazil: Journal of South American Earth Sciences, v. 103, https://doi.org/10.1016/j.jsames.2020.102738.

Tozer, B., Sandwell, D.T., Smith, W.H.F., Olson, C., Beale, J.R., and Wessel, P., 2019, Global bathymetry and topography at 15 Arc Sec: SRTM15+: Earth and Space Science, v. 6, p. 1847–1864, https://doi.org/10.1029/2019EA000658.

Xia, Y., Kopp, H., Klaeschen, D., Geersen, J., Ma, B., and Schnabel, M., 2023, Seamount and ridge subduction at the Java Margin, Indonesia: Effects on structural geology and seismogenesis: Journal of Geophysical Research: Solid Earth, v. 128, https://doi.org/10.1029/2022JB026272.

Printed in the USA

Downloaded from pubs.geoscienceworld.org/gsa/geology/article-pdf/54/10/1027/8317041/g54871.1.pdf by RWTH Aachen University user on 17 November 2026